Data acquisition and processing of distributed full-waveform induced polarization exploration

*Weiqiang Liu[1], Rujun Chen[2]**
[1] College of Geophysics, China University of Petroleum-Beijing, Beijing, 102249, China
2 School of Geosciences and Info-Physics, Central South University, Changsha, 410083, China

Summary

Induced polarization (IP) is an effective geophysical method for characterizing near-surface complex resistivity structures. To improve the precision and efficiency of massive-scale exploration, a large-scale distributed full-waveform IP system is developed and an intelligent signal processing technology is proposed for the first time. The testing of practical data show that IP data quality can be extremely improved by distributed acquisition and anti-interference processing.

Introduction

The IP effect is an electrochemical phenomenon produced in a multiphase medium under the action of an electric field, which includes electric polarization (conductive minerals) and thin-film polarization (non-conductive minerals) (Seigel et al 2007; Johansson et al 2020; Gross et al 2021; Revil et al 2021). In practical, rocks, animals, and plant micro-organisms are all multi-phase media, the IP exploration can be used to identify the physical characteristics of them (including composition, structure, structure, porosity, permeability, salinity, conductive mineral content, and so on) (Ahmed et al 2019; Martin et al 2021; Wang et al 2021). In addition, the IP effect can also be considered in various electromagnetic explorations, such as transient electromagnetic (TEM), controlled source audio magnetotelluric (CSAMT), airborne electromagnetic (AEM), and so on (Madsen et al 2020; Zhou et al 2020).

Recently, IP measurements of various rock and ore samples have been achieved in the laboratory. However, Observing IP response at the low-frequency band (10^{-3}~10^{-1} Hz) is challenging and difficult in practical field surveys, because of low working efficiency and strong electromagnetic interference. Transmitting a long-period exciting current and observing a long-period synchronous IP signal can take a long time. Additionally, electromagnetic (EM) interferences caused by natural and artificial sources at low frequency are strong, which may distort most of the data, so in practical exploration, IP data are mainly observed at 0.1 Hz~100 Hz and even higher frequencies. However, Acquiring IP data at low frequency is also necessary, because of two points. First, many ore deposits, carbonaceous slate, and other sedimentary strata can be discriminated by using the complex resistivity spectrum at low frequency. Second, the electromagnetic coupling effect is an inherent interference in IP survey, which is weak at low frequency and can be removed by linear correction.

An effective method to improve observation efficiency is developing three-dimensional distributed observation systems. There has been great progress in instrument development (Alfouzan et al 2020; Li et al 2020). Many research institutions and companies have developed the distributed instruments, such as MIMDAS IP system in Australia, Newmont distributed acquisition system (NEWDAS) in the United States, Quantec's 3D system in Canada, IRIS full-waver instrument in French. However, large-scale field observing and anti-interference processing of IP data at low frequencies are still challenges and research hotspots (Olsson et al 2016; Liu et al 2016, 2017, 2019; Barfod et al 2021). In this paper, we developed a distributed full-waveform induced polarization exploration system, which can realize 50-200 nodes (corresponding 200-800 channels) IP exploration with real-time full-waveform data acquisition constraint, which is one of the largest-scale IP exploration systems in China. Since the system mainly transmits spread spectrum signals, rather than square wave signal, it was named as spread spectrum induced polarization (SSIP) system. Additionally, a complete signal de-noising method is also proposed.

Theory and/or Method

The distributed IP system consists of two parts: transmitter and receiver. The transmitter includes a digital generator (which can stably transmit 220V alternating current), an intelligent transformer and rectifier (output voltage is 0-1000V), a pseudo-random signal conditioner (which can modulate two kinds of spread-spectrum signals, 2n sequence and m sequence). The range of signal frequency can reach 1/1024-8192 Hz by combining waveforms of different bandwidths. The transmitter uses GPS for synchronization, the synchronization accuracy is less than 30 ns. The system power consumption is less than 1 W. The receiver is based on the Zigbee and wireless sensor network autonomous networking. The current electrodes and potential electrodes are completely separated to avoid electromagnetic induction and coupling. A PC with a ZigBee adapter is used to control the data acquisition and monitor the data quality. Data acquisition software includes control center run on portable personal computer (PC) and data acquisition unit (DAU) software run on IP data acquisition station (DAS). The control center software is composed of a user interface (UI) module, DAU management module, DAU agent module and communication module. Based on the GPS

DOI:10.1190/iceg2021-069.1

synchronization, ZigBee and wireless sensor network, the IP system can realize the simultaneous collection of 200 sets of 800 channels.

Electromagnetic interference mainly includes: low-frequency trend item interference caused by telluric current, discontinuous interference by machinery and equipment in mines, outliers caused by spike interference, and electromagnetic coupling interference caused by electromagnetic induction of the earth. In order to improve the precision and efficiency of large-scale data processing, an automatic signal processing technology based on a de-noising library and the statistical decision is proposed for the first time. To deal with various kinds of electromagnetic interferences in electrical exploration, five signal processing techniques including: empirical mode decomposition, waveform matching analysis, robust statistics, principal component analysis and wavelet analysis, are improved and integrated as a de-noising method library. Then, a statistical decision tree is established to automatically identify the noise interference and select the corresponding signal processing method, according to the statistical information of the original time series in each survey point. The statistical information including the mean value, standard deviation, outlier ratio, noise to signal ratio, current-voltage correlation of every segment. The change of mean value in each segment represents the trend drift disturbance. The distribution of standard deviation and correlation reflects strong burst noise interference. The distribution of outliers per period reflects the existence of spike interference. The noise ratio can reflect the strength of background Gaussian noise. The synthetic algorithm is verified by simulated data. Finally, after de-noising, apparent IP parameters are estimated and 3D inversion is performed.

Examples

We analysed the data acquisition and processing of the SSIP full-waveform IP in a mining area in Southern China. The sample frequency is 64 Hz, the period is 256 s, and the fundamental frequency is 0.0039 Hz, observing time is over an hour. Complex resistivity at 1/256 Hz, 2/256 Hz, 4/256 Hz, 8/256 Hz, 16/256 Hz can be calculated after signal processing of the time domain IP series. In this survey area, about 50 survey lines with 100 survey points per line were arranged using scanning and sounding arrangements separately. The survey line distance is 40 m and the survey point distance is 20 m. Potential electrode space MN is 20 m. For scanning arrangement, current electrode space AB is 5000 m. For sounding arrangement, AB is 300 m, 600 m, 900 m, 1200 m, 1500 m, 1800 m, 2100 m, 2400 m, 2700 m, 3000 m, 3300 m, 3600 m and 3900 m separately. Typically, the max probe depth is 1/3~1/6 of the max AB. Almost all the full-waveform IP data are threatened by electromagnetic interference caused by artificial and natural sources. Fig. 1 shows the schematic diagram of distributed full-waveform IP data acquisition of part of the survey points in the field.

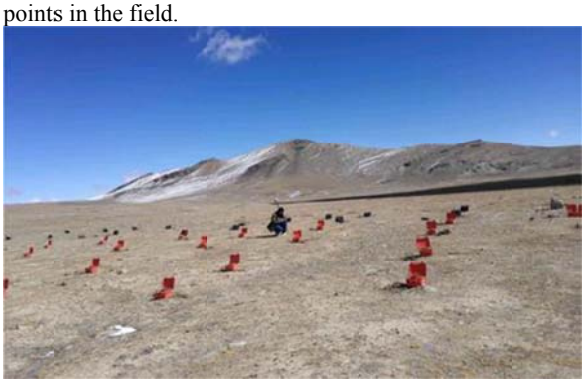

Figure 1: Schematic diagram of distributed full-waveform IP data acquisition in the field.

Based on the anti-interference processing algorithm, a high-quality 3D complex resistivity data set of more than 5000 survey points are obtained. We show part of the data set to analyze the effect. Fig. 2 shows a planar contour map of the apparent resistivity and phase at 1/256 Hz, using IP scanning data (current electrode AB=5000 m). Resistivity data were determined by the primary field, so they are less disturbed by the noises. However, the phase data were determined by the secondary field, so they were greatly interfered by the noises, and the phase map was distorted seriously. After de-noising, the distortion disappeared. An IP anomaly area with low-resistivity and high-phase can be traced out on the upper-right side of the contour maps, which was inferred as a lead-zinc ore metallogenic favorable area combined with other geological and borehole materials.

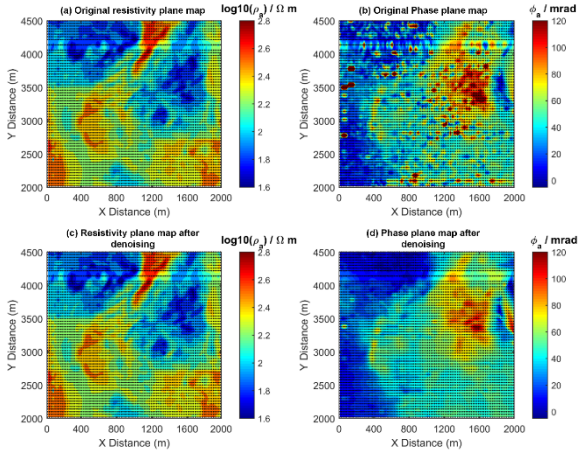

Figure 2: Contour maps of apparent resistivity and apparent phase plane obtained at 1/256 Hz for 5000 surveying points with and without de-noising processing.

DOI:10.1190/iceg2021-069.1

Conclusions

Based on the development of IP theory and technology, a distributed full-waveform SSIP instrument system and a complete anti-interference data processing method was proposed. This method was applied to a large-scale spread-spectrum practical data acquired in a mining area in Southern China. The data quality was improved greatly. The distortions in the complex resistivity phase were removed by comparing the results with and without anti-interference processing. This application in large-scale detection demonstrates that anti-interference processing is effective to improve the data quality in practical IP exploration, especially for large-space and low-frequency detection.

Acknowledgments

The research is supported by China Postdoctoral Science Foundation (2021M693492), Science Foundation of China University of Petroleum, Beijing (2462020YJRC010, 2462020YXZZ005) and the Key Laboratory of Geophysical Electromagnetic Probing Technologies of Ministry of Natural Resources (KLGEPT201908).

References

Ahmed, A. S., Revil, A., and Gross, L. 2019. Multiscale induced polarization tomography in hydrogeophysics: A new approach. Advances in Water Resources, 134, 103451.

Alfouzan, F. A., Alotaibi, A. M., Cox, L. H., and Zhdanov, M. S. 2020. Spectral induced polarization survey with distributed array system for mineral exploration: case study in Saudi Arabia. Minerals, 10, 769.

Barfod, A. S., Lévy, L., and Larsen, J. J. 2021. Automatic processing of time domain induced polarization data using supervised artificial neural networks. Geophysical Journal International, 224, 312-325.

Gross, L., Ahmed, A. S., and Revil, A. 2021. Induced polarization of volcanic rocks. 4. Large-scale induced polarization imaging. Geophysical Journal International, 225, 950–967.

Johansson, S., Lindskog, A., Fiandaca, G., and Dahlin, T. 2020. Spectral induced polarization of limestones: time domain field data, frequency domain laboratory data and physicochemical rock properties. Geophysical Journal International, 220, 928-950.

Li, W., Zhang, Q., Luo, Y., Zhang, Q., and Jiang, F. 2020. Development of a new multifunctional induced polarization instrument based on remote wireless communication technology. IEEE Access, 8, 100415-100425.

Liu, W., Chen, R., Cai, H., & Luo, W. 2016. Robust statistical methods for impulse noise suppressing of spread spectrum induced polarization data, with application to a mine site, Gansu province, China. Journal of Applied Geophysics, 135, 397-407.

Liu, W., Chen, R., Cai, H., Luo, W., & Revil, A. 2017. Correlation analysis for spread-spectrum induced-polarization signal processing in electromagnetically noisy environments. Geophysics, 82(5), E243-E256.

Liu, W., Lü, Q., Chen, R., Lin, P., Chen, C., Yang, L., and Cai, H. 2019. A modified empirical mode decomposition method for multiperiod time-series detrending and the application in full-waveform induced polarization data. Geophysical Journal International, 217, 1058-1079.

Madsen, L. M., Fiandaca, G., and Auken, E. 2020. 3-D time-domain spectral inversion of resistivity and full-decay induced polarization data—full solution of Poisson's equation and modelling of the current waveform. Geophysical Journal International, 223, 2101-2116.

Martin, T., Titov, K., Tarasov, A., and Weller, A. 2021. Spectral induced polarization: frequency domain versus time domain laboratory data. Geophysical Journal International, 225, 1982-2000.

Olsson, P. I., Fiandaca, G., Larsen, J. J., Dahlin, T., Auken, E. 2016. Doubling the spectrum of time-domain induced polarization by harmonic de-noising, drift correction, spike removal, tapered gating and data uncertainty estimation. Geophysical Journal International, 207, 774-784.

Revil, A., Qi, Y., Ghorbani, A., Gresse, M., and Thomas, D. M. 2021. Induced polarization of volcanic rocks. 5. Imaging the temperature field of shield volcanoes. Geophysical Journal International, 225, 1492-1509.

Seigel, H., Nabighian, M., Parasnis, D. S., and Vozoff, K. 2007. The early history of the induced polarization method. The Leading Edge, 26, 312-321.

Wang, C., Binley, A., and Slater, L. D. 2021. On negative induced polarization in frequency domain measurements. Geophysical Journal International, 225, 342-353.

Zhou, N. N., Kangxin, L., Xue, G., and Chen, W. 2020. Induced polarization effect on grounded-wire transient electromagnetic data from transverse electric and magnetic fields. Geophysics, 85, E111-E120.